

## Article

# Seismic Performance Target and Fragility of Masonry Infilled RC Frames under In-Plane Loading

Chunhui Liu <sup>1,2</sup>, Bo Liu <sup>1</sup>, Xiaomin Wang <sup>3,4,\*</sup>, Jingchang Kong <sup>1,\*</sup>  and Yuan Gao <sup>1</sup><sup>1</sup> School of Civil Engineering, Yantai University, Yantai 264005, China<sup>2</sup> Department of Civil and Environmental Engineering, University of Alberta, Edmonton, AB T6G 2R3, Canada<sup>3</sup> Key Laboratory of Earthquake Engineering and Engineering Vibration, Institute of Engineering Mechanics, China Earthquake Administration, Harbin 150080, China<sup>4</sup> Key Laboratory of Earthquake Disaster Mitigation, Ministry of Emergency Management, Harbin 150080, China

\* Correspondence: xiaomin\_wang@iem.ac.cn (X.W.); kjch8811@126.com (J.K.)

**Abstract:** Masonry infilled RC frames are one of the most common structural forms, the damage of which, in earthquake events, usually cause serious losses. The determination of the seismic performance target is the key foundation of performance-based seismic evaluation and design for masonry infilled RC frames. In this paper, an extensive database of experimental tests on infilled RC frames loaded in an in-plane direction is collated. According to the crack propagation and elastic-plastic characteristics of infilled RC frames, the damage process is divided into four stages, and then the criteria of the damage states (DS) are proposed. In addition, the seismic performance targets expressed as inter-story drift ratio (IDR) for the four stages are suggested, which would support the performance-based in-plane seismic analysis of infilled RC frames. Finally, the proposed in-plane seismic performance target is utilized to analyze the fragility of two masonry infilled RC frame structures.

**Keywords:** masonry infilled RC frame; in-plane seismic performance target; damage state (DS); inter-story drift ratio (IDR); fragility analysis



**Citation:** Liu, C.; Liu, B.; Wang, X.; Kong, J.; Gao, Y. Seismic Performance Target and Fragility of Masonry Infilled RC Frames under In-Plane Loading. *Buildings* **2022**, *12*, 1175. <https://doi.org/10.3390/buildings12081175>

Academic Editors: Weiping Wen and Duofa Ji

Received: 13 July 2022

Accepted: 2 August 2022

Published: 6 August 2022

**Publisher's Note:** MDPI stays neutral with regard to jurisdictional claims in published maps and institutional affiliations.



**Copyright:** © 2022 by the authors. Licensee MDPI, Basel, Switzerland. This article is an open access article distributed under the terms and conditions of the Creative Commons Attribution (CC BY) license (<https://creativecommons.org/licenses/by/4.0/>).

## 1. Introduction

Masonry infills are one of the most prevalent types of nonstructural elements used in modern architecture buildings in both China and abroad [1]. The existence of infill walls not only changes the stiffness and strength of the structural system and its distribution, but also adversely affects the local restraint conditions of the main structural members [2,3]. The collapse of infill walls can cause significant property damage, and may even affect emergency evacuation and endanger life safety [4–8]. Nonetheless, infill walls are considered to be non-structural components in most countries of the world, and the interaction between infill walls and frames is ignored when designing reinforced concrete (RC) frame structures. On the contrary, the seismic performance assessment of infill wall RC frames requires the consideration of non-structural components [9–11]. Therefore, the seismic response of masonry infills should be reliably characterized to accurately analyze the seismic performance of the overall structure under different damage states (DSs).

Some researchers [12–15] utilized the degree and severity of cracking patterns observed on panels, or the failure typology of brick units, to define the different DSs. Others [14], on the other hand, related such DSs with the infilled RC frame peak load, or the achievement of given strength reduction ratios. In general, the in-plane damage of infill walls was divided into three or four stages in the literature [12–23]. The definition of inter-story drift ratio (IDR) thresholds and their uncertainty corresponding to specific physical damage levels on infill walls has been the subject of various research studies [13–15,24,25]. Some researchers [26,27] proposed IDR limits for frame structures with infill walls corresponding

to different DSs based on test data, which provided a basis for seismic code. Chiozzi [15] collected a large amount of infill wall test data, classified the DS of infill walls by quantifying the crack width, and proposed the corresponding IDR thresholds. Zhang [21] gave the IDR limits for infill walls at different DSs by summarizing the damage modes and characteristics of infill walls and referring to the existing performance index.

In this paper, an extensive database of experimental tests on infilled RC frames loaded in an in-plane direction is collated. The in-plane DS of an infilled RC frame is divided into four stages by considering both in-plane mechanical properties and the observed damage of infill walls. The seismic performance targets expressed as inter-story drift ratio (IDR) for the four stages are suggested. Finally, the seismic performance targets are applied to analyze the fragility of two masonry infilled RC frame structures.

## 2. Database of Experimental Tests

The first step of the present research was the collection of a database of tests on infilled RC frames. 132 experimental results of masonry infilled RC frames loaded in an in-plane direction, in 46 studies completed over the last four decades, were collected. The chronological distribution of these studies is shown in Figure 1, and the details are described in Table 1. The research parameters in these studies vary, including, for example, different openings and masonry materials. The selected infills in this paper are ordinary masonry walls without special reinforcement and openings, which are loaded by lateral in-plane cyclic loading through actuators.

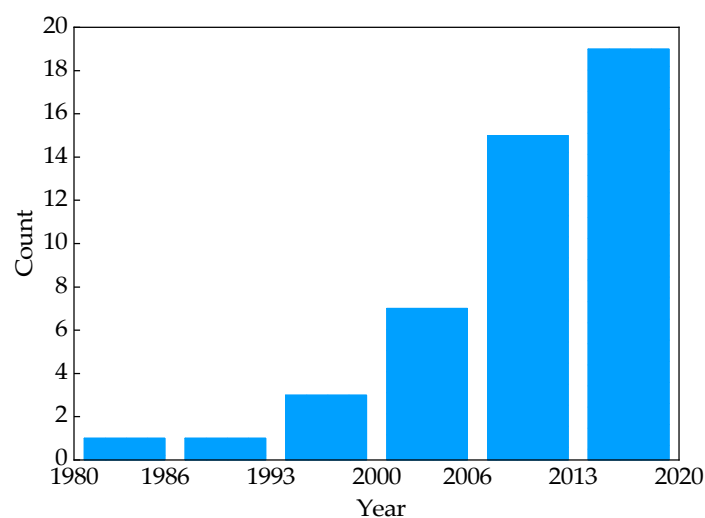


**Figure 1.** Chronological distribution of the literature.

**Table 1.** The details of the literature.

Number	Literatures	Number of Selected Tests	Research Parameters
1	Xiong (2013) [28]	4	axial compression ratio, opening
2	Sun, et al. (2005) [29]	1	masonry material
3	Shi, et al. (1996) [27]	1	opening
4	Angel, et al. (1994) [30]	5	in-plane damage
5	Cavaleri, et al. (2014) [31]	1	masonry material
6	Chiou, et al. (2015) [32]	2	Height, axial compression ratio
7	Colangelo (2005) [33]	6	in-plane damage
8	Haider (1995) [34]	3	in-plane damage
9	Mansouri, et al. (2014) [35]	1	opening
10	Misir, et al. (2015) [36]	1	masonry material

Table 1. Cont.

Number	Literatures	Number of Selected Tests	Research Parameters
11	Pereira, et al. (2011) [37]	1	masonry material
12	Schwarz, et al. (2015) [38]	5	height-width ratio
13	Sabouri-Ghomi, et al. (2017) [39]	3	boundary condition
14	Žarnić, et al. (1984) [40]	1	masonry material
15	Vasconcelos, et al. (2015) [41]	1	loading method
16	Zovkic, et al. (2013) [42]	1	masonry material
17	Huang (2011) [43]	5	masonry material, height-width ratio
18	Li, et al. (2015) [44]	1	boundary condition, masonry material
19	Gu, et al. (2010) [45]	5	masonry material
20	Jiang, et al. (2009) [46]	2	panel reinforcement
21	Lin, et al. (2018) [47]	4	masonry material
22	Zhou, et al. (2015) [48]	1	boundary condition, wall-filling rate
23	Su, et al. (2017) [49]	1	opening
24	Cheng, et al. (2013) [50]	1	opening
25	Lin (2019) [51]	4	masonry material
26	Li (2013) [52]	1	masonry material
27	Xiong, et al. (2017) [53]	2	masonry material
28	Tang, et al. (2012) [54]	5	number of layers, spans
29	Kakaletsis, et al. (2007) [55]	1	opening
30	Yang, et al. (2008) [56]	2	height-width ratio, opening, constructional column
31	Hao, et al. (2008) [57]	3	height-width ratio
32	Zhang, et al. (2007) [58]	2	masonry material
33	Wu, et al. (2016) [59]	1	masonry material
34	Zhan (2001) [60]	6	mortar strength
35	Wang, et al. (2003) [61]	1	prestress
36	Zhao (2005) [62]	1	Reinforcement, constructional column
37	Liao, et al. (2018) [63]	3	masonry material
38	Cheng, et al. (2005) [64]	2	constructional column
39	Xia (2004) [65]	5	boundary condition
40	Dautaj, et al. (2018) [66]	7	frame strength
41	Alwashali, et al. (2019) [67]	5	concrete strength, mortar strength
42	Cheng, et al. (1989) [68]	8	masonry material, opening
43	Bergami, et al. (2015) [69]	2	with or without block
44	Calvi, et al. (2008) [70]	2	in-plane damage
45	Gazić, et al. (2016) [71]	5	masonry material, mortar strength
46	C. Stylianidis (2012) [72]	7	strengthening

### 3. Seismic Performance Targets of Infilled RC Frame

In this section, the four damage stages are defined according to the damage status. The damage process of the collected infilled RC frame specimens under increasing in-plane lateral displacements is analyzed. The IDR value can reflect the damage degree of the infill walls statistically. Finally, the IDR value corresponding to each DS is determined.

#### 3.1. Definition of Damage States (DSs)

In recent years, different definitions of DSs have been proposed. Some definitions, such as the one in study [15] (shown in Table 2), are about macroscopic damage descriptions, and do not consider the mechanical properties of the infill wall. Although these definitions can facilitate people to take appropriate repair measures, they easily make people infer different understanding. Other definitions, which relate the DSs to the mechanical properties of the infilled RC frame, can facilitate researchers in studying the performance of infilled RC frames. However, the lack of a damage phenomena description makes it difficult to apply in a practical earthquake event.

**Table 2.** Definition of DSs in literature [15].

Damage Stage	Brief Description
DS1	Minor cracks at the junction of the wall, gray joints or wall frames, no damage to blocks, no slippage in cracks
DS2	Wall extension mortar joints or blocks with obvious cracks greater than 2mm, local block crushing, and cracks with small slips appear
DS3	Large cracks appear, the crack width is generally greater than 4mm, cracks have obvious slippage, masonry unit large area crushing and spalling

In this study, the test process of each collected infilled RC frame is analyzed, considering the cracking degree, block and mortar damage, the applied in-plane loads and lateral displacement of the infilled specimen. The DS is divided into four stages, considering both the damage description and the mechanical properties of the infill walls. The main characteristics of each stage are described as follows:

In the DS1 stage, there are no obvious cracks in the infill wall. Even if there are small cracks, they can restore to the original state immediately after unloading. There is no damage in the frame members and the infill wall is well connected to the frame. The load-displacement curve is almost linear, and the stiffness is constant in this stage, which is the elastic stage.

In the DS2 stage, the diagonal cracks at the corners of the wall increase, the widths of which expand and cannot restore to their original state after unloading. Different cracks begin to connect to each other gradually through the whole wall. The plaster layer of the wall spalls and falls down slightly. There are some tiny cracks in the columns and beams. In this stage, the infilled RC frame gradually develops to the elastic-plastic stage.

In the DS3 stage, cracks increase and develop into an X shape. The appearance of penetration cracks results in the division of the wall and the falling of broken blocks. Cracks in the columns and beams increase, and the infill wall is detached from the frame at the top corners. The structural plasticity develops further in this stage. The maximum lateral load is reached.

In the DS4 stage, many broken masonry segments fall down and the wall is severely damaged. Cracks in the beams and columns are enlarged and plastic hinges appear in the structural member ends. In this stage, in order to avoid the completed detachment of the wall from the frame and the wall collapse, the test is generally stopped while the applied load decreases to 80% of the peak capacity. A brief description of the four DSs is described in Table 3.

**Table 3.** Definition of DSs in this paper.

Stage	State	Elastic/Plastic State	Infill Wall State	RC Frame State	Definition
DS1	Basically intact	Elastic	No cracks to small cracks	Intact	No cracks to small cracks
DS2	Slight damage	Elastic-plastic	Inclined cracks appear and gradually penetrate the wall, and mortar peels off at the cracks	Tiny cracks	Small cracks to Penetration cracks
DS3	Moderate damage	Plastic	Corner damage blocks fall down, and the cracks develop into an X shape	Increased cracks	Penetration cracks to peak load
DS4	Severe damage	Failed	Mass shedding of mortar and broken blocks	Beam and column yield and plastic hinges appear	Peak load to infill collapse

### 3.2. IDR Limits at DSs of Each Test

IDR is a suitable index for reflecting the in-plane damage state of infill walls [13–15]. According to the assumed damage state definition, the IDR values related to the four DSs are listed for each specimen in Table 4. Due to the lack of descriptive details in the literature,

some information for the four damage states of specimens cannot be obtained. Therefore, some IDR values are not given in Table 4, which is indicated by '-'. Moreover, due to the uncertainty of wall damage in the actual test, the data of some tests deviate from most of the test results (see Figure 2). In order not to affect the accuracy of the statistical results, individual points with a large dispersion are excluded, which is represented in Table 4 with a bold font; a total of four points were removed.

**Table 4.** IDR values at each DS.

#	Reference	Label	DS1(%)	DS2(%)	DS3(%)	DS4(%)
1		W-1	0.39	-	0.93	2.00
2		W-2	0.39	-	0.82	1.26
3	Xiong (2013) [28]	W-3	0.47	-	1.11	1.34
4		W-4	0.63	-	1.52	2.41
5	Sun, et al. (2005) [29]	RCF	0.08	-	2.13	3.39
6	Shi, et al. (1996) [27]	Infill wall frame	0.04	0.21	0.79	3.33
7		2a	0.17	-	-	-
8		3a	0.11	-	-	-
9	Angel, et al. (1994) [30]	6a	0.13	-	-	-
10		7a	0.13	-	-	-
11		8a	0.20	-	-	-
12	Cavaleri, et al. (2014) [31]	s1b2	-	-	0.50	1.53
13		B39L	0.13	0.50	-	2.00
14	Chiou, et al. (2015) [32]	B83T	0.13	0.50	-	2.00
15		C1	0.03	0.05	-	1.42
16		C2	0.02	0.11	-	-
17		L1	0.03	0.16	-	1.63
18	Colangelo (2005) [33]	L2	0.03	0.16	-	2.28
19		N1	-	-	0.21	2.03
20		N2	0.03	-	0.20	2.16
21		A1	0.25	-	-	2.50
22	Haider (1995) [34]	B1	0.25	-	-	2.50
23		D2	0.25	-	-	2.50
24	Mansouri, et al. (2014) [35]	S	0.05	-	-	3.50
25	Misir, et al. (2015) [36]	SWF	-	-	-	-
26	Pereira, et al. (2011) [37]	Ref_Wall	-	-	0.20	-
27		1000	0.33	-	1.20	2.67
28		1100	0.10	-	0.30	2.33
29	Schwarz, et al. (2015) [38]	0000	-	-	0.70	2.67
30		0100	0.33	-	0.40	4.00
31		0101	-	-	1.20	-
32		CU2	0.05	-	-	1.01
33	Sabouri-Ghomi, et al. (2017) [39]	CU5	0.06	-	-	1.23
34		CU6	0.07	-	-	1.38
35	Žarnić, et al. (1984) [40]	M2	0.11	-	-	-
36	Vasconcelos, et al. (2015) [41]	2	0.11	-	1.15	1.43
37	Zovkic, et al. (2013) [42]	Model 3	0.06	-	-	-
38		AFKJ1	0.20	0.33	4.40	<b>4.00</b>
39		AFKJ2	0.10	0.20	2.20	4.00
40	Huang (2011) [43]	AFKJ3	0.10	0.14	1.69	4.00
41		AFKJ4	0.10	0.14	4.40	<b>4.00</b>
42		AFKJ5	0.10	0.50	4.40	<b>4.00</b>
43	Li, et al. (2015) [44]	W2	0.06	-	1.62	-
44		PD10-5-0.6	0.13	-	0.18	0.25
45		PD10-10-0.6	0.19	-	0.28	0.36
46	Gu, et al. (2010) [45]	PM-0.3	0.10	-	0.15	0.20
47		PM-0.6	0.04	-	0.35	0.37
48		PM-0.9	0.26	-	0.35	0.37
49		F2	0.09	0.22	-	-
50	Jiang, et al. (2009) [46]	F3	0.10	0.19	-	-

Table 4. Cont.

#	Reference	Label	DS1(%)	DS2(%)	DS3(%)	DS4(%)
51		IF1	0.19	0.33	0.94	1.61
52		IF2	0.06	0.20	0.62	1.56
53	Lin, et al. (2018) [47]	IF3	0.19	0.33	0.47	1.68
54		IF4	0.06	0.20	1.52	2.68
55	Zhou, et al. (2015) [48]	GWF2	0.13	0.14	1.80	3.09
56	Su, et al. (2017) [49]	HBF-1	0.04	-	0.25	0.37
57	Cheng, et al. (2013) [50]	MWF-11	-	-	0.61	1.02
58		IF1	0.18	0.30	0.91	1.46
59		IF2	0.09	0.13	0.76	1.66
60	Lin (2019) [51]	IF5	0.06	0.18	1.82	2.85
61		IF6	0.18	0.30	0.68	1.88
62	Li (2013) [52]	Infill wall RC frame	0.14	0.27	0.70	1.10
63		KJQ-1	0.13	0.53	1.43	2.46
64	Xiong, et al. (2017) [53]	KJQ-3	0.09	0.48	0.78	1.49
65		GPF-1	0.01	0.50	1.44	2.68
66		MGPF-0	0.17	-	1.96	2.66
67	Tang, et al. (2012) [54]	MGPF-1	0.01	-	0.58	1.20
68		MGPF-2	0.06	-	0.86	2.72
69		MGPF-3	0.07	-	1.09	2.63
70	Kakaletsis, et al. (2007) [55]	S	-	-	0.83	1.20
71		W-1a	0.35	-	0.77	0.90
72	Yang, et al. (2008) [56]	W-3a	0.16	-	0.39	0.52
73		W-5	0.03	-	0.22	0.30
74	Hao, et al. (2008) [57]	W-6	0.03	-	0.20	0.33
75		W-7	0.04	-	0.17	0.67
76		KZ1	0.08	0.77	-	-
77	Zhang, et al. (2007) [58]	KZ2	0.07	-	-	-
78	Wu, et al. (2016) [59]	QKJ	0.09	0.23	-	-
79		W5.0-1	0.12	-	0.27	0.54
80		W5.0-2	0.06	0.18	0.27	-
81		W5.0-3	0.05	0.07	0.33	-
82	Zhan (2001) [60]	W7.5-1	0.12	0.15	0.18	-
83		W7.5-2	0.05	0.08	0.11	-
84		W7.5-3	0.02	0.05	0.08	-
85	Wang, et al. (2003) [61]	W1	0.16	-	0.67	1.33
86	Zhao (2005) [62]	ZS-1	0.05	-	0.21	0.35
87		M-1	0.12	1.45	2.69	-
88	Liao, et al. (2018) [63]	M-2	0.09	0.67	2.87	-
89		M-3	0.07	0.48	0.71	-
90		CZ-1	0.10	-	-	0.14
91	Cheng, et al. (2005) [64]	CZ-2	0.09	-	-	<b>0.09</b>
92		A1	0.09	-	0.19	-
93		A2	0.08	-	0.19	-
94	Xia (2004) [65]	A3	0.12	-	1.08	-
95		B2	0.13	-	1.03	-
96		B3	0.70	-	1.18	-
97		2	0.30	0.30	1.90	6.00
98		6	0.26	0.26	1.28	6.00
99		8	0.18	0.18	1.38	5.25
100	Dautaj, et al. (2018) [66]	9	0.16	0.16	1.50	-
101		10	0.24	-	1.48	-
102		11	0.11	-	1.35	-
103		13	0.28	-	1.88	-
104		F-0.4	0.10	-	0.80	-
105		F-0.6	0.08	0.10	0.50	-
106	Alwashali, et al. (2019) [67]	F-1.5	-	-	0.60	-
107		WM	0.10	-	0.60	-
108		WB	0.10	-	0.70	-

Table 4. Cont.

#	Reference	Label	DS1(%)	DS2(%)	DS3(%)	DS4(%)
109		QZ-TJ-02	0.03	-	0.17	-
110		QZ-TJ-01	0.05	-	0.20	-
111		QZ-TJ-04	0.06	-	0.29	-
112	Cheng, et al. (1989) [68]	QZ-TJ-03	0.03	-	0.17	-
113		QZ-TJ-09	0.02	-	0.14	-
114		QZ-TJ-14	0.02	-	0.28	-
115		QZ-TJ-13	0.04	-	0.27	-
116		QZ-TJ-15	0.03	-	0.25	-
117		Bergami, et al. (2015) [69]	FT1	0.16	-	1.21
118	FT2		0.09	-	1.08	-
119	Calvi, et al. (2008) [70]	2	0.06	0.18	-	-
120		6	0.06	0.20	-	-
121		O3 bpm	0.16	-	-	-
122		O4 bpm	0.18	-	-	-
123	Gazić, et al. (2016) [71]	O1 bpm	0.11	-	-	-
124		O1 bvm	0.06	-	-	-
125		O1 bpm *	0.05	-	-	-
126		F1,1,6	0.12	0.31	0.81	-
127		FN1,1,6	0.06	0.28	0.73	-
128		F1,1,9	0.14	0.31	0.81	-
129	C. Stylianidis (2012) [72]	FN1,1,9	0.08	0.31	0.81	-
130		FN1	0.07	0.28	0.72	-
131		FN2	0.09	0.31	0.81	-
132		FN6	0.20	0.83	2.15	-

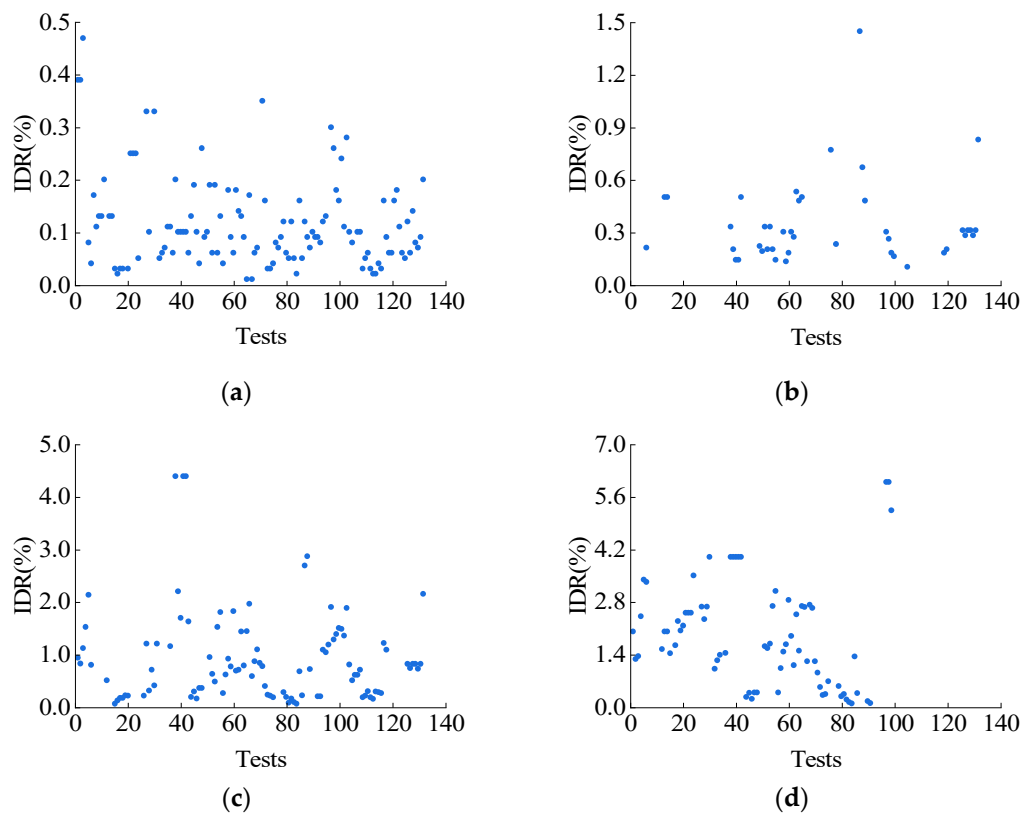


Figure 2. Scatter diagram of IDR at each DS. (a) DS1; (b) DS2; (c) DS3; (d) DS4.

### 3.3. Seismic Performance Target

A drift-based fragility function is utilized in this paper, to estimate the probability of a given damage state occurring in the RC frame under a specific level of drift. The definition of the fragility function usually adopts a lognormal cumulative distribution function, as shown in Equation (1).

$$P[\text{DS} \geq \text{ds}_i | \text{IDR}_j] = \Phi\left(\frac{\ln(\text{IDR}_j) - \mu_i}{\beta_i}\right) \quad (1)$$

where  $P[\text{DS} \geq \text{ds}_i | \text{IDR}_j]$  is the conditional probability that the component will experience or exceed the  $i$ th DS given the inter-story drift value  $\text{IDR}_j$ ;  $\Phi(\cdot)$  is the standard normal cumulative distribution function;  $\mu_i$  is the logarithmic mean value; and  $\beta_i$  is the logarithmic standard deviation. The fragility function curves for the four DSs are shown in Figure 3.

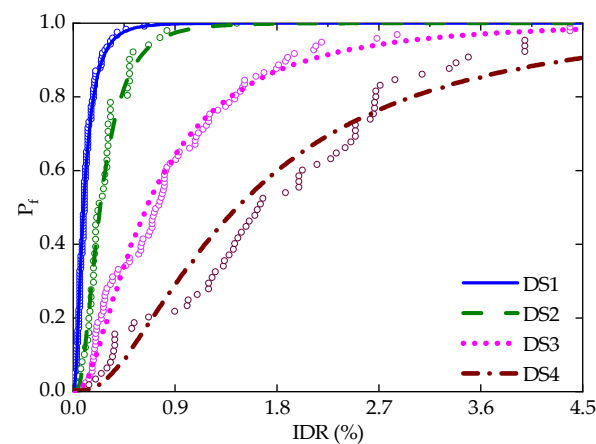


Figure 3. Proposed fragility function curves for infill panels.

According to the proposal by Chiozzi et al. [15], the mean values of the  $\text{IDR}$ ,  $\overline{\text{IDR}}$ , for the four DSs, are chosen as the in-plane seismic performance target of the infilled RC frame, which is shown in Table 5. The statistical parameters  $\mu$  and  $\beta$  for the fitted log-normal probability distribution for each DS are listed in Table 5 as well, where  $\mu = \text{mean}(\ln(\text{IDR}))$ .

Table 5. Seismic performance target and statistical parameters.

Damage State	$\overline{\text{IDR}}$	$\mu$	$\beta$
DS1	0.1%	−2.3718	0.7952
DS2	0.3%	−1.4255	0.6818
DS3	0.9%	−0.4275	0.9039
DS4	1.9%	0.3626	0.8590

## 4. Fragility Analysis of Masonry Infilled RC Frames

### 4.1. Design of Structures

In order to assess the seismic fragility of infilled RC frames, two RC frames with four and eight stories were designed according to the Chinese seismic design code [73]. The four-story structure had a site category of II and a design seismic group of III. The eight-story structure had a site category of III and a design seismic group of I. They both had a seismic intensity of eight degrees (0.2 g), a site characteristic period of 0.45 s, and a seismic grade of II. The design load information of the two RC frame structures is shown in Table 6. Figure 4 shows their elevations with the infill walls. The infill wall was made of concrete hollow block with a strength grade of MU10, the size of which was 390 mm × 190 mm × 190 mm. The beam and column cross-sections of the two RC frame structures

and material information are shown in Table 7. The detailed design information can be found in the literature [74].

**Table 6.** Design loads information.

Category	Dead Load (kN/m <sup>2</sup> )		Live Load (kN/m <sup>2</sup> )		The Thickness of Slab (mm)	
	4-Story	8-Story	4-Story	8-Story	4-Story	8-Story
Room	1.5	2	2.0	2.5	100	120
Corridor	1.5	2	3.5	3.5	100	120
Roof	5.5	3	0.4	2	120	120

Note: The dead load does not include the floor weight.

**Table 7.** Cross-section of beams and columns and material information.

Floor	Beam (mm)	Column (mm)	The Stirrup Ratio of Beam	The Stirrup Ratio of Column	Concrete Grades	Steel Bars Grades	
4-story	1~4	500 × 500	400 × 300	0.5%	0.3%	C30	HRB400
8-story	1	Side	800 × 800	0.3%	0.8%	C50	
	2~3	Middle				C45	
	4					C30	
	5~8	500 × 500				650 × 650	C30

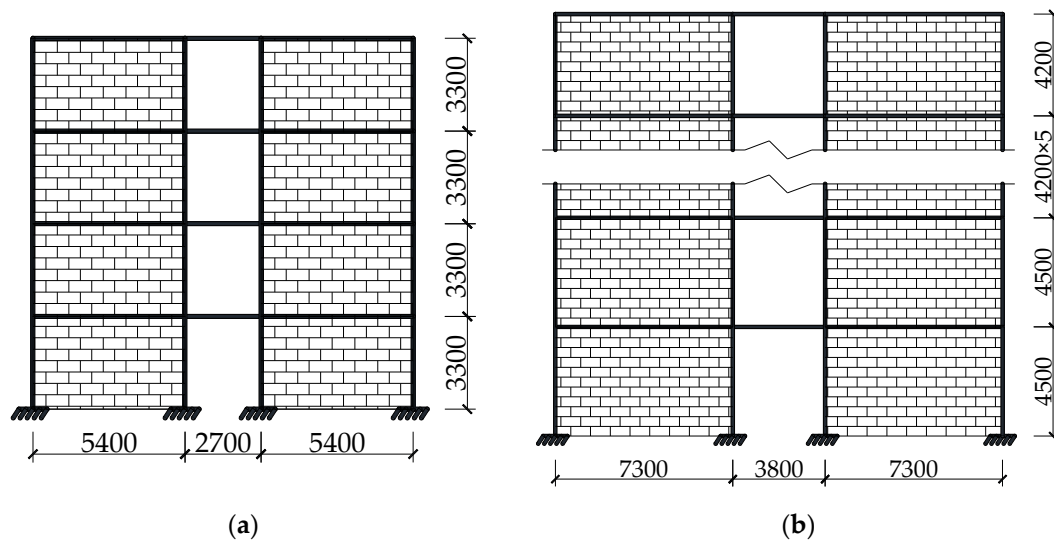


**Figure 4.** Elevation of infilled RC frame structure (Unit: mm). (a) 4-story structure; (b) 8-story structure.

#### 4.2. Modeling of Infilled RC Frame

The numerical models of infilled RC frame structures were created utilizing the OpenSees platform. The RC beams and columns were simulated using nonlinear beam-column elements, the cross-section of which was simulated using a force-based fiber section model. The Concrete02 material model was used to simulate the properties of concrete, and the core concrete strength was calculated using the modified Scott–Kent–Park model. The Steel02 material model was used to simulate the properties of steel reinforcement, the strain-hardening ratio of which was taken as 0.01. The geometric nonlinear analysis of the frame columns was achieved by setting up a local coordinate transformation considering the  $P$ - $\Delta$  effect.

The infill wall was simulated using an equivalent single brace model, which was represented by the Pinching4 uniaxial material model [75] shown in Figure 5. This material

model can be used to simulate materials with pinching load-deformation response and degradation under cyclic loading. Its skeleton curve can be determined by referring to the method proposed by Liberatore et al. [76]. The skeleton curve model of infill, shown in Figure 6, is described by a multilinear curve with the following four characteristic points:  $(d_{40}, 0.40 V_p)$ ,  $(d_{85}, 0.85 V_p)$ ,  $(d_p, V_p)$ , and  $(d_c, 0)$ .  $V_p$  is the peak load and  $d_p$  is the corresponding displacement;  $d_{40}$  and  $d_{85}$  are the displacement corresponding to 40% and 80% of the peak load; and  $d_c$  is the displacement when the load decreases to zero. These parameters are calculated using Equations (2)–(8) through regression analysis [76]. This model does not take into account the residual strength of the infill wall, but in this paper the residual strength is set as 10% of the peak load [77]. The corresponding residual displacement  $d_u$  is calculated by Equation (9). Finally, the values of the four key points  $(\$ePd_1, \$ePf_1)$ ,  $(\$ePd_2, \$ePf_2)$ ,  $(\$ePd_3, \$ePf_3)$ , and  $(\$ePd_4, \$ePf_4)$  of the Pinching4 material model are  $(d_{40}, 0.40 V_p)$ ,  $(d_{85}, 0.85 V_p)$ ,  $(d_p, V_p)$ , and  $(d_u, 0.1 V_p)$ , respectively.

$$d_{40} = \theta_{40} h_m \quad (2)$$

$$d_{85} = 1.04(d_{40} + \Delta\theta_{85} h_m) \quad (3)$$

$$d_p = 1.07(d_{40} + \Delta\theta_{85} h_m + \Delta\theta_p h_m) \quad (4)$$

$$d_c = 1.05(d_{40} + \Delta\theta_{85} h_m + \Delta\theta_p h_m + 0.9\Delta\theta_c h_m) \quad (5)$$

$$V_{40} = \alpha_V V_{p,0} \quad (6)$$

$$V_{p,0} = \tau_{h,eff} t l_m \quad (7)$$

$$\frac{V_{p,0}}{t l_m f_{mk}} = \frac{\tau_{h,eff}}{f_{mk}} = \frac{0.269}{f_{mk}^{0.641}} \quad (8)$$

$$d_u = 0.9d_c + 0.1d_p \quad (9)$$

where  $\theta_{40}$  represents the drift ratio corresponding to 40% of the strength;  $\Delta\theta_{85}$ ,  $\Delta\theta_p$  and  $\Delta\theta_c$  are the drift ratio increments; coefficient  $\alpha_V$  is a correction factor, which is taken here as 0.98;  $h_m$ ,  $l_m$  and  $t$  are the height, width and thickness of the infill wall respectively; and  $f_{mk}$  is the compressive strength of the masonry.

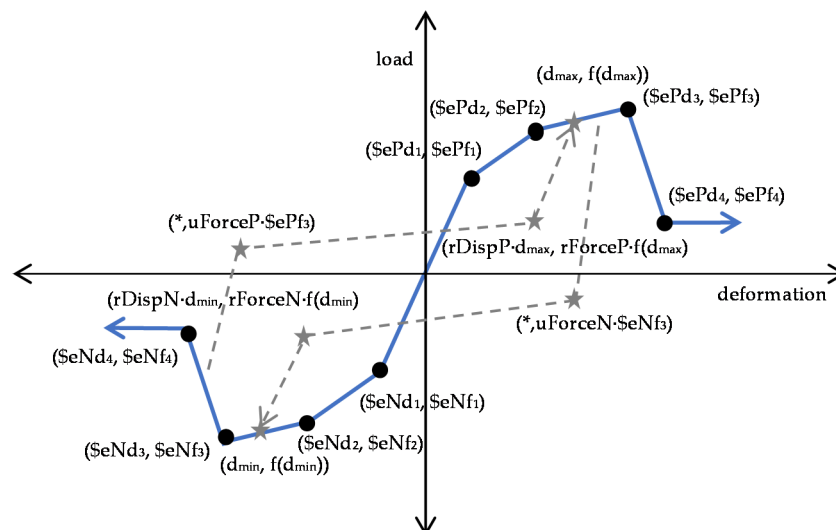
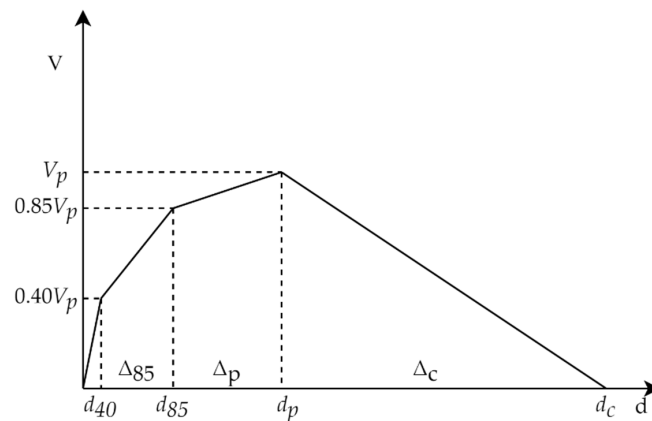


Figure 5. Pinching4 uniaxial material model [75].



**Figure 6.** The skeleton curve model of infill.

Then, the parameters of the hysteretic rule of the Pinching4 uniaxial material model were determined according to the research of Blasi et al. [78] and Kumar et al. [79], as follows:

$$\begin{aligned}
 [rDispP \quad rForceP \quad uForceP] &= [rDispN \quad rFprceN \quad uForceN] = [0.5 \quad 0.1 \quad -0.05] \\
 \begin{bmatrix} gK1 & gK2 & gK3 & gK4 & gKLim \\ gD1 & gD2 & gD3 & gD4 & gDLim \\ gF1 & gF2 & gF3 & gF4 & gFLim \\ gE \end{bmatrix} &= \begin{bmatrix} 0.5 & 0.2 & 0.3 & 0.2 & 0.9 \\ 0.1 & 0.1 & 2.0 & 2.0 & 0.5 \\ 0.1 & 0.1 & 1.0 & 1.0 & 0.9 \\ 10 \end{bmatrix}
 \end{aligned}$$

where  $rDispP$ ,  $rForceP$ ,  $uForceP$ ,  $rDispN$ ,  $rFprceN$ , and  $uForceN$  are the scaling factors that control the pinching of materials;  $gK1$ ,  $gK2$ ,  $gK3$ ,  $gK4$ , and  $gKLim$  control the cyclic degradation model for unloading stiffness degradation;  $gD1$ ,  $gD2$ ,  $gD3$ ,  $gD4$ , and  $gDLim$  control the cyclic degradation model for reloading stiffness degradation;  $gF1$ ,  $gF2$ ,  $gF3$ ,  $gF4$ , and  $gFLim$  control the cyclic degradation model for strength degradation; and  $gE$  is used to define maximum energy dissipation under cyclic loading.

#### 4.3. Selected Ground Motions

The 22 remote ground motion records recommended by FEMA P695 (ATC-63) [80] were selected for incremental dynamic analysis (IDA). Since each record has two directions, a total of 44 records were used for the analysis. The selected earthquake intensity was the spectral acceleration  $Sa$  for a ground motion record at the fundamental period of structures, which was calculated with 5% viscous damping. The acceleration spectra of 44 ground motions and the mean acceleration spectra are shown in Figure 7.

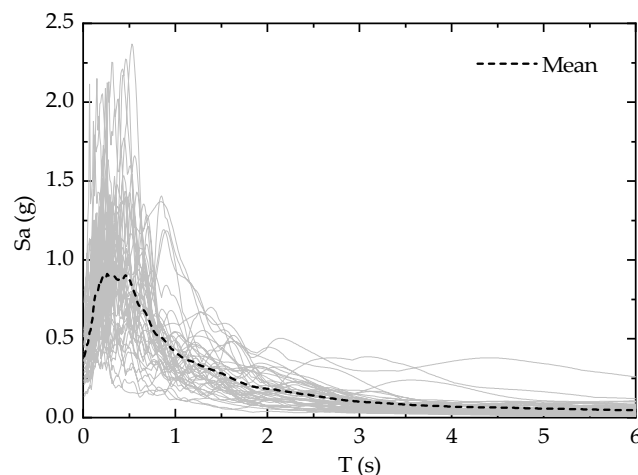


**Figure 7.** The acceleration spectra of the selected 44 ground motions.

#### 4.4. Structure Fragility Analysis

The seismic fragility of structures refers to the probability of reaching a certain damage state or performance level under seismic excitations of different intensities. The definition of structure fragility function also adopts a lognormal cumulative distribution function, the parameters of which have different meanings from Equation (1), as shown in Equation (10).

$$P[EDP \geq edp_i | IM] = \Phi \left( \frac{\ln(IM) - \mu_{EDP|IM}}{\beta_{EDP|IM}} \right) \tag{10}$$

where  $P[EDP \geq edp_i | IM]$  is the conditional probability that a ground motion will cause the structure to reach the  $i$ th damage state;  $EDP$  is the seismic response of the structure, which in this paper is the maximum IDR of the structure;  $edp_i$  is the seismic capacity of the structure corresponding to the IDR value for each DS determined in the previous section;  $IM$  is the seismic intensity index, which is defined in this paper as the spectral acceleration corresponding to the structural period of ground motion records;  $\mu_{EDP|IM}$  is the logarithmic mean value; and  $\beta_{EDP|IM}$  is the logarithmic standard deviation.

The incremental dynamic analyses were conducted for the four-story and eight-story RC frame structures with infill walls introduced in Section 4.1, and the IDA curves obtained are shown in Figure 8. The fragility curves of each DS, determined by Equation (10), are shown in Figure 9.

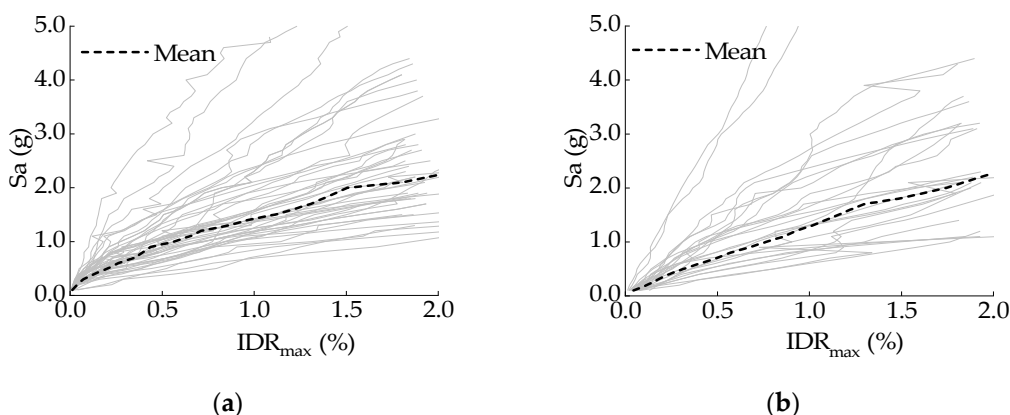


Figure 8. The IDA curves of the two structures: (a) 4-story; (b) 8-story.

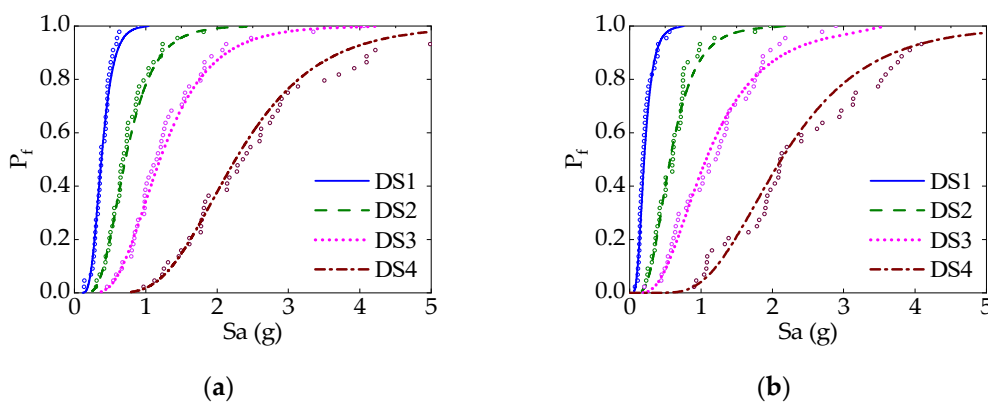


Figure 9. The fragility curves of the two structures: (a) 4-story; (b) 8-story.

The probability of the two structures reaching DS1 was 79% and 97%, respectively, when  $S_a$  was 0.5 g. Meanwhile, the probability of the two structures reaching DS2 was 20% and 40%, respectively, when  $S_a$  was 0.5 g. The probability of the two structures reaching DS3 was 3% and 9%, respectively, when  $S_a$  was 0.5 g. However, reaching DS4

was challenging for the two structures, which required ground motion intensity several times larger. The probability of the four-story structure reaching DS4 was 79%, 20% and 3%, requiring Sa 3.1 g, 1.6 g and 1.1 g, respectively. The probability of the eight-story structure reaching DS4 was 97%, 40% and 9%, requiring Sa 4.82 g, 1.9 g and 1.2 g, respectively.

The fragility curves of the structure in Figure 9 flattened as the structures reached DS1 to DS4, i.e., the probability of transcendence became progressively smaller. The DS1 curves in the figure are the steepest and the structures reached DS1 when Sa was very small, indicating that the structure could easily break through the DS1 limit to reach DS2 under a low seismic action. The DS4 curves are the flattest, which required a larger Sa for the same transcendence probability, indicating that it was difficult for the structures to reach DS4.

## 5. Conclusions

In this paper, a definition of the damage state of infill walls loaded in an in-plane direction was developed. A corresponding performance target was proposed, which was applied to carry out a fragility analysis of two infilled RC frames.

First, an extensive database of experimental tests on infilled RC frames stressed by in-plane loading was collected and presented. The in-plane damage state (DS) of infill walls was defined as four stages according to the observed damage process as well as the mechanical properties during the test. The IDR values corresponding to each DS were identified, and fitted to the lognormal distribution function. The parameters of the lognormal fragility functions corresponding to each DS were obtained. The mean value of the IDR was chosen as the performance target of each DS, which was 0.1%, 0.3%, 0.9% and 1.9%, respectively.

Then, the proposed seismic performance targets were used to conduct a fragility analysis of two infilled wall RC frames. The probability of the four-story structure reaching DS1, DS2 and DS3 was 79%, 20% and 3%, respectively, when Sa was 0.5 g. However, the probability of the four-story structure reaching DS4 was 79%, 20% and 3%, requiring Sa 3.1 g, 1.6 g and 1.1 g, respectively. The results demonstrated that the infilled RC frame structures could reach DS1 and DS2 under a relatively low seismic intensity. When the seismic intensity increased, DS3 could be reached gradually. However, reaching DS4 was challenging, which required ground motion intensity several times larger.

It should be noted that the conclusions obtained in this study are related to the data collected due to the empirical IDR value. In the future, more effort will be made to expand the experimental database and the out-of-plane seismic performance target of the infill walls. Furthermore, the overall seismic performance of infilled RC frames under bidirectional seismic motions should be researched as well.

**Author Contributions:** Conceptualization, C.L. and X.W.; methodology, X.W.; software, B.L. and X.W.; validation, C.L., B.L. and J.K.; formal analysis, B.L.; investigation, C.L. and Y.G.; resources, C.L. and J.K.; data curation, B.L. and Y.G.; writing—original draft preparation, B.L.; writing—review and editing, C.L. and X.W.; visualization, B.L.; supervision, J.K.; project administration, J.K. funding acquisition, C.L. and J.K. All authors have read and agreed to the published version of the manuscript.

**Funding:** This research was funded by the National Nature Science Foundation of China (Nos. 51908484 and 51808478), and the Natural Science Foundation of Shandong (Nos. ZR2019QEE033). These supports are greatly appreciated.

**Institutional Review Board Statement:** Not applicable.

**Informed Consent Statement:** Not applicable.

**Acknowledgments:** Grateful acknowledgment is given to Liang Cui and Jinkai Ma at the School of Civil Engineering, Yantai University, for their guidance and suggestions on theoretical analyses.

**Conflicts of Interest:** The authors declare no conflict of interest.

## References

1. Shah, S.A.A.; Shahzada, K.; Samiullah, Q. Influence of Brick Masonry Infilled Wall on Seismic Performance of Reinforced Concrete Frame. *NED Univ. J. Res.* **2020**, *17*, 15–29. [[CrossRef](#)]
2. Khan, N.; Monti, G.; Nuti, C.; Vailati, M. Effects of Infills in the Seismic Performance of an RC Factory Building in Pakistan. *Buildings* **2021**, *11*, 276. [[CrossRef](#)]
3. Mazza, F.; Donnici, A. In-plane-out-of-plane single and mutual interaction of masonry infills in the nonlinear seismic analysis of RC framed structures. *Eng. Struct.* **2022**, *257*, 114076. [[CrossRef](#)]
4. Zhai, C.H.; Wang, X.M.; Kong, J.C.; Wei, Y.L.; Jin, W.; Zhao, Y. Progress and prospect of seismic performance of masonry-infilled RC frames. *J. Harbin Inst. Technol.* **2018**, *50*, 1–13. [[CrossRef](#)]
5. Demirel, I.O.; Yakut, A.; Binici, B. Seismic performance of mid-rise reinforced concrete buildings in Izmir Bayrakli after the 2020 Samos earthquake. *Eng. Fail. Anal.* **2022**, *137*, 106277. [[CrossRef](#)]
6. Mazza, F. Base-isolation of a hospital pavilion against in-plane-out-of-plane seismic collapse of masonry infills. *Eng. Struct.* **2021**, *228*, 111504. [[CrossRef](#)]
7. Malla, S.; Karanjit, S.; Dangol, P.; Gautam, D. Seismic Performance of High-Rise Condominium Building during the 2015 Gorkha Earthquake Sequence. *Buildings* **2019**, *9*, 36. [[CrossRef](#)]
8. Bai, J.; He, J.; Li, C.; Jin, S.; Yang, H. Experimental investigation on the seismic performance of a novel damage-control replaceable RC beam-to-column joint. *Eng. Struct.* **2022**, *267*, 114692. [[CrossRef](#)]
9. Furtado, A.; Teresa de Risi, M. Recent Findings and Open Issues concerning the Seismic Behaviour of Masonry Infill Walls in RC Buildings. *Adv. Civ. Eng.* **2020**, *2020*, 9261716. [[CrossRef](#)]
10. Arumugam, V.; Keshav, L.; Achuthan, A.; Dasappa, S.; Chelladurai, S.J.S. Seismic Evaluation of Advanced Reinforced Concrete Structures. *Adv. Mater. Sci. Eng.* **2022**, *2022*, 4518848. [[CrossRef](#)]
11. Adhikari, R.; Rupakhety, R.; Giri, P.; Baruwal, R.; Subedi, R.; Gautam, R.; Gautam, D. Seismic Fragility Analysis of Low-Rise RC Buildings with Brick Infills in High Seismic Region with Alluvial Deposits. *Buildings* **2022**, *12*, 72. [[CrossRef](#)]
12. Baggio, C.; Bernardini, A.; Colozza, R.; Corazza, L.; Della Bella, M.; Di Pasquale, G.; Dolce, M.; Goretti, A.; Martinelli, A.; Orsini, G. *Field Manual for Post-Earthquake Damage and Safety Assessment and Short Term Countermeasures (AeDES)*; European Commission—Joint Research Centre—Institute for the Protection and Security of the Citizen, EUR, 22868; European Commission: Brussels, Belgium, 2007.
13. Colangelo, F. Drift-sensitive non-structural damage to masonry-infilled reinforced concrete frames designed to Eurocode 8. *Bull. Earthq. Eng.* **2013**, *11*, 2151–2176. [[CrossRef](#)]
14. Cardone, D.; Perrone, G. Developing fragility curves and loss functions for masonry infill walls. *Earthq. Struct.* **2015**, *9*, 257–279. [[CrossRef](#)]
15. Chiozzi, A.; Miranda, E. Fragility functions for masonry infill walls with in-plane loading. *Earthq. Eng. Struct. Dyn.* **2017**, *46*, 2831–2850. [[CrossRef](#)]
16. Kong, J.C.; Zhai, C.H.; Li, S.; Xie, L.L. Study on in-plane seismic performance of solid masonry-infilled RC frames. *China Civ. Eng. J.* **2012**, *45*, 137–141. [[CrossRef](#)]
17. Zhai, C.H.; Kong, J.C.; Wang, X.M.; Chen, Z.Q. Experimental and Finite Element Analytical Investigation of Seismic Behavior of Full-Scale Masonry Infilled RC Frames. *J. Earthq. Eng.* **2016**, *20*, 1171–1198. [[CrossRef](#)]
18. ASCE. *Seismic Rehabilitation of Existing Buildings*; American Society of Civil Engineers: Reston, VA, USA, 2007.
19. He, A.; Zhao, Z.Z. Study on fragility of autoclaved aerated concrete block infills. *Earthq. Eng. Eng. Dyn.* **2020**, *40*, 178–185. [[CrossRef](#)]
20. Liu, J.Y. Performance-Based Seismic Evaluation for Infilled Frames. Master's Thesis, Xi'an University of Architecture and Technology, Xi'an, China, 2008.
21. Zhang, M.Y. Components Performance-Based Seismic Vulnerability Analysis of Masonry infilled Frame Structures. Master's Thesis, Institute of Engineering Mechanics, China Earthquake Administration, Harbin, China, 2017.
22. FEMA. *Prestandard and Commentary for the Seismic Rehabilitation of Buildings*; FEMA P356; Federal Emergency Management Agency: Washington, DC, USA, 2000.
23. GB/T 24335-2009; Classification of Earthquake Damage to Buildings and Special Structures. Institute of Engineering Mechanics, C.E.A: Harbin, China, 2009.
24. Masi, A.; Manfredi, V.; Cetraro, G. In-plane performance of RC infilled frames under seismic actions: Experimental versus code provision values. In *Brick and Block Masonry—Trends, Innovations and Challenges*; Modena, C., da Porto, F., Valluzzi, M.R., Eds.; CRC Press: Boca Raton, FL, USA, 2016.
25. Sassun, K.; Sullivan, T.J.; Morandi, P.; Cardone, D. Characterising the in-plane seismic performance of infill masonry. *Bull. N. Z. Soc. Earthq. Eng.* **2016**, *49*, 98–115. [[CrossRef](#)]
26. Tong, Y.S.; Qian, G.F. Deformation Behavior and Load Capacity of Reinforced Concrete Frames with Brick Filled Walls. *J. Xi'an Univ. Archit. Technol. Nat. Sci. Ed.* **1985**, *17*, 1–21.
27. Shi, Q.X.; Tong, Y.S.; Qian, G.F. Earthquake response analysis for reinforced concrete frames with masonry filler walls. *J. Xi'an Univ. Archit. Technol. Nat. Sci. Ed.* **1996**, *28*, 71–75.
28. Xiong, H. The Research on Analysis of Frame Filled Wall under Seismic Action. Master's Thesis, Hunan University, Changsha, China, 2013.

29. Sun, Y.D.; Xiao, J.Z.; Zhou, D.Y.; Zhang, P. Experimental research on seismic behavior of recycled concrete frame filled with recycled lightweight masonry blocks. *Earthq. Eng. Eng. Dyn.* **2005**, *25*, 126–133. [[CrossRef](#)]
30. Angel, R.; Abrams, D.; Shapiro, D.; Uzarski, J.; Webster, M. *Behavior of Reinforced Concrete Frames with Masonry Infills*; University of Illinois Engineering Experiment Station, College of Engineering, University of Illinois at Urbana-Champaign: Champaign, IL, USA, 1994.
31. Cavaleri, L.; Di Trapani, F. Cyclic response of masonry infilled RC frames: Experimental results and simplified modeling. *Soil Dyn. Earthq. Eng.* **2014**, *65*, 224–242. [[CrossRef](#)]
32. Chiou, T.C.; Hwang, S.J. Tests on cyclic behavior of reinforced concrete frames with brick infill. *Earthq. Eng. Struct. Dyn.* **2015**, *44*, 1939–1958. [[CrossRef](#)]
33. Colangelo, F. Pseudo-dynamic seismic response of reinforced concrete frames infilled with non-structural brick masonry. *Earthq. Eng. Struct. Dyn.* **2005**, *34*, 1219–1241. [[CrossRef](#)]
34. Haider, S. In-Plane Cyclic Response of Reinforced Concrete Frames with Unreinforced Masonry Infills. Master's Thesis, Rice University, Houston, TX, USA, 1995.
35. Mansouri, A.; Marefat, M.S.; Khanmohammadi, M. Experimental evaluation of seismic performance of low-shear strength masonry infills with openings in reinforced concrete frames with deficient seismic details. *Struct. Des. Tall Spec. Build.* **2014**, *23*, 1190–1210. [[CrossRef](#)]
36. Misir, I.S.; Ozelik, O.; Girgin, S.C.; Yucel, U. The Behavior of Infill Walls in RC Frames Under Combined Bidirectional Loading. *J. Earthq. Eng.* **2015**, *20*, 559–586. [[CrossRef](#)]
37. Pereira, M.F.P.; Pereira, M.; Ferreira, J.; Lourenço, P.B. Behavior of masonry infill panels in RC frames subjected to in plane and out of plane loads. In Proceedings of the 7th International Conference AMCM 2011, Krakow, Poland, 13–15 June 2011.
38. Schwarz, S.; Hanaor, A.; Yankelevsky, D.Z. Experimental Response of Reinforced Concrete Frames with AAC Masonry Infill Walls to In-plane Cyclic Loading. *Structures* **2015**, *3*, 306–319. [[CrossRef](#)]
39. Sabouri-Ghomi, S.; Payandehjoo, B. Analytical and Experimental Studies of the Seismic Performance of Drawer Bracing System (DBS). *Int. J. Civ. Eng.* **2017**, *15*, 1087–1096. [[CrossRef](#)]
40. Žarnić, R.; Tomazevic, M. *Study of the Behavior of Masonry Infilled Reinforced Concrete Frames Subjected to Seismic Loading—Part One*; Report ZRMK/IKPI-84/04; Institute for Testing and Research in Materials and Structures: Ljubljana, Yugoslavia, 1984.
41. Vasconcelos, G.; Akhoundi, F.; Lourenço, P.B.; Palha, C.; Silva, L. In-plane and out-of plane experimental characterization of RC masonry infilled frames. In Proceedings of the 6th International Conference on Mechanics and Materials in Design, Ponta Delgada, Portugal, 26–30 July 2015.
42. Zovkic, J.; Sigmund, V.; Guljas, I. Cyclic testing of a single bay reinforced concrete frames with various types of masonry infill. *Earthq. Eng. Struct. Dyn.* **2013**, *42*, 1131–1149. [[CrossRef](#)]
43. Huang, Q.X. Study on Seismic Behavior and Elastic-Plastic Analysis Method for Seismic Responses of RC Frame Infilled with New Masonry. Ph.D. Thesis, Huaqiao University, Quanzhou, China, 2011.
44. Li, J.H.; Xue, Y.T.; Xiao, C.Z.; Chang, Z.Z.; Li, Y. Experimental study on seismic performance of full-scale RC frame infilled with autoclaved aerated concrete blocks. *China Civ. Eng. J.* **2015**, *48*, 12–18. [[CrossRef](#)]
45. Gu, X.L.; CHEN, G.L.; Ma, J.Y.; Li, X. Experimental study on mechanical behavior of concrete perforated brick walls under cyclic loading. *J. Build. Struct.* **2010**, *31*, 123–131. [[CrossRef](#)]
46. Jiang, L.X.; Zheng, Q.W. Tests of seismic behavior of reinforced concrete frames with infilled wall or strengthened infilled wall. *Ind. Constr.* **2009**, *39*, 40–47. [[CrossRef](#)]
47. Lin, C.; Guo, Z.X.; Huang, Q.X.; Ye, Y.; Chai, Z.L.; Liu, Y. Experimental study on seismic behavior of full-scale infilled RC frames. *J. Build. Struct.* **2018**, *39*, 30–37. [[CrossRef](#)]
48. Zhou, X.J.; Li, Z.X.; Xu, D.D.; Jiang, X.L. Experiment on Seismic Behavior of Flexible Connection Masonry Infilled Frame Structure. *J. Tianjin Univ. Sci. Technol.* **2015**, *48*, 155–166. [[CrossRef](#)]
49. Su, Q.W.; Zhang, Y.; Xu, Z.Y.; Cai, H.R. Full-Scale Tests on Seismic Behavior of RC Frames Infilled with Hollow Bricks. *J. SouthWest Jiaotong Univ.* **2017**, *52*, 532–539. [[CrossRef](#)]
50. Cheng, J.T.; Tang, X.R. Nonlinear finite element analysis of reinforced concrete frame structures with opening masonry infilled wall. *J. Suzhou Univ. Sci. Technol. Eng. Technol.* **2013**, *26*, 24–27.
51. Lin, C. Seismic Performance and Interaction Mechanism of Infilled RC Frames Using New Masonry Blocks. Ph.D. Thesis, Huaqiao University, Quanzhou, China, 2019.
52. Li, X.D. Experimental and Analytical Study of Seismic Performance of Lightweight Masonry-Infilled RC Frames. Master's Thesis, Harbin Institute of Technology, Harbin, China, 2013.
53. Xiong, F.; Wang, P.; Zhang, W.B.; Chen, J. Experimental Study on the Seismic Behavior of RC Frame with Fiber Gypsum Infilled Wall. *Adv. Eng. Sci.* **2017**, *49*, 1–9. [[CrossRef](#)]
54. Tang, X.R.; Zhou, Z.Y.; Liu, L.H.; Yang, L. Experimental study on seismic behavior of multi-story masonry infilled reinforced concrete frame structures. *J. Build. Struct.* **2012**, *33*, 72–81. [[CrossRef](#)]
55. Kakaletsis, D.; Karayannis, C. Experimental investigation of infilled r/c frames with eccentric openings. *Struct. Eng. Mech.* **2007**, *26*, 231–250. [[CrossRef](#)]
56. Yang, W.J.; Chen, L.Q.; Zhu, X.Q. Experimental study on seismic behavior of concrete perforated brick walls. *Eng. Mech.* **2008**, *25*, 126–133.

57. Hao, T.; Liu, L.X.; Wang, R.Y. Experimental study on seismic performance of concrete perforated brick wall. *Struct. Units Units Archit.* **2008**, *22*–25.
58. Zhang, Y.T.; Shen, D.M. Quasi-static Experimental Study on Concrete Perforated Brick Wall. *Build. Struct.* **2007**, *3*, 91–93. [[CrossRef](#)]
59. Wu, F.B.; Zhu, H.F.; Ouyang, J.; Jiang, W.; Zhou, X.H. Experiment on Seismic Behavior of Concrete Horizontal-hole Hollow Blocks Infilled Wall-RC Frames. *J. Archit. Civ. Eng.* **2016**, *33*, 7–13.
60. Zhan, H. Experimental Research on the Seismic Behavior and Shear-Bearing Capacity of the Walls Made of KP1 Burned Shale-Farinoscoal Porous Bricks. Master's Thesis, Hunan University, Changsha, China, 2001.
61. Wang, Y.H.; Ai, J.; Zhang, C.F.; Lv, Z.T. Experimental study on prestressed concrete block wall under low cyclic reversed loading. *Build. Struct.* **2003**, *4*, 3–7. [[CrossRef](#)]
62. Zhao, Q.B. Experimental Research on the Improvement of Seismic Behavior of Load Bearing Masonry made of Autoclaved Aerated Concrete. Master's Thesis, Tianjin University, Tianjin, China, 2005.
63. Liao, Q.; Li, B.X.; Shi, Y.X.; Meng, C.Y. Experimental study on seismic performance of RC frames filled with lightweight wallboards. *J. Build. Struct.* **2018**, *39*, 44–51. [[CrossRef](#)]
64. Cheng, C.Y.; Wu, M.S. Experimental study on seismic performance of yitong aerated concrete masonry wall. In Proceedings of the 2005 National Masonry Structure Basic Theory and Engineering Application Conference, Shanghai, China, 17 December 2005; pp. 99–104.
65. Xia, G.M. Testing Study on Anti-Seismic Behavior of the Masonry Walls of Nonbearing Anti-Seismic Energy-Saving Bliocks. Master's Thesis, Dalian University of Technology, Dalian, China, 2004.
66. Dautaj, A.D.; Kadir, Q.; Kabashi, N. Experimental study on the contribution of masonry infill in the behavior of RC frame under seismic loading. *Eng. Struct.* **2018**, *165*, 27–37. [[CrossRef](#)]
67. Alwashali, H.; Sen, D.; Jin, K.; Maeda, M. Experimental investigation of influences of several parameters on seismic capacity of masonry infilled reinforced concrete frame. *Eng. Struct.* **2019**, *189*, 11–24. [[CrossRef](#)]
68. Cheng, C.Y.; Zhu, B.L.; Wang, X.M.; Zheng, Y. Seismic performance of lime-sand brick wall under low cyclic loading. *Sichuan Build. Sci.* **1989**, 5–9.
69. Bergami, A.V.; Nuti, C. Experimental tests and global modeling of masonry infilled frames. *Earthq. Struct.* **2015**, *9*, 281–303. [[CrossRef](#)]
70. Calvi, G.M.; Bolognini, D. Seismic Response of Reinforced Concrete Frames Infilled with Weakly Reinforced Masonry Panels. *J. Earthq. Eng.* **2008**, *5*, 153–185. [[CrossRef](#)]
71. Gazić, G.; Sigmund, V. Cyclic testing of single-span weak frames with masonry infill. *Grđevinar* **2016**, *68*, 617–633.
72. Stylianidis, K.C. Experimental Investigation of Masonry Infilled R/C Frames. *Open Constr. Build. Technol. J.* **2012**, *6*, 194–212. [[CrossRef](#)]
73. GB 50011-2010; Code for Seismic Design of Buildings. Ministry of Housing and Urban-rural Construction of the People's Republic of China: Beijing, China, 2010.
74. Yan, Q.X. Seismic Resilience Assessment of RC Frame Structure Considering Mainshock-Aftershock Effect. Master's Thesis, Harbin Institute of Technology, Harbin, China, 2021.
75. Pinching4 Material. Available online: [https://opensees.berkeley.edu/wiki/index.php/Pinching4\\_Material](https://opensees.berkeley.edu/wiki/index.php/Pinching4_Material) (accessed on 20 May 2022).
76. Liberatore, L.; Noto, F.; Mollaioli, F.; Franchin, P. In-plane response of masonry infill walls: Comprehensive experimentally-based equivalent strut model for deterministic and probabilistic analysis. *Eng. Struct.* **2018**, *167*, 533–548. [[CrossRef](#)]
77. Furtado, A.; Rodrigues, H.; Arêde, A. Modelling of masonry infill walls participation in the seismic behaviour of RC buildings using OpenSees. *Int. J. Adv. Struct. Eng.* **2015**, *7*, 117–127. [[CrossRef](#)]
78. Blasi, G.; De Luca, F.; Aiello, M.A. Brittle failure in RC masonry infilled frames: The role of infill overstrength. *Eng. Struct.* **2018**, *177*, 506–518. [[CrossRef](#)]
79. Kumar, M.; Rai, D.C.; Jain, S.K. Ductility Reduction Factors for Masonry-Infilled Reinforced Concrete Frames. *Earthq. Spectra* **2015**, *31*, 339–365. [[CrossRef](#)]
80. FEMA. *Quantification of Building Seismic Performance Factors*; FEMA P695; Federal Emergency Management Agency: Washington, DC, USA, 2009.